

Asymmetry of the magnetization reversal mechanism probed by relaxation measurements in La-Ca-Mn-O ferromagnetic/antiferromagnetic multilayers

I. Panagiotopoulos,^{1,2} N. Moutis,¹ and C. Christides³

¹*Institute of Materials Science, National Center for Scientific Research "Demokritos," 153 10 Athens, Greece*

²*Department of Materials Science and Engineering, University of Ioannina, 45 110 Ioannina, Greece*

³*Department of Engineering Sciences, School of Engineering, University of Patras, 26 110 Patras, Greece*

(Received 13 September 2001; published 19 March 2002)

In exchange-coupled ferromagnetic/antiferromagnetic $\text{La}_{0.60}\text{Ca}_{0.40}\text{MnO}_3$ (FM)/ $\text{La}_{0.33}\text{Ca}_{0.67}\text{MnO}_3$ (AF) multilayers the magnetization reversal mechanism is probed by magnetic viscosity and remanence measurements below (5 K) and above (80 K) the blocking temperature $T_B = 70$ K. The magnetic relaxation follows the $\ln(t)$ behavior at 5 K, which is a universal feature of a slow relaxation process, whereas at 80 K the time decay requires an additional exponential term. Below T_B , the observed loop asymmetries in the irreversible susceptibility (χ_{irr}) and the magnetic viscosity (S) reveal two inequivalent reversal mechanisms between the field increasing and field decreasing branches of the hysteresis loop.

DOI: 10.1103/PhysRevB.65.132407

PACS number(s): 75.70.Cn, 81.15.Fg, 72.15.Gd, 75.30.Gw

The construction of complex layered structures¹ that consist of $\text{La}_{0.67}\text{A}_{0.33}\text{MnO}_3$ ($\text{A} = \text{Ca}, \text{Sr}$) ferromagnetic (FM) perovskites is one of the hottest topics in magnetism today due to ever increasing demand for nanostructured sensors and magnetic storage nanodevices.² The exchange bias phenomenon,³ through which the exchange coupling between a FM and an antiferromagnetic (AF) layer can cause a unidirectional anisotropy at the FM/AF interface, is often used⁴ in thin-film devices to pin the magnetization in a desired direction. Exchange biasing can be observed when the FM layer is field cooled through the Neel temperature of the AF phase and it appears as a displaced FM hysteresis loop. Today there are a lot of questions that remain open in understanding the intriguing microscopic reversal mechanisms in exchange-biased films where a large variety of interfacial spin structures can be stabilized.^{3,5,6} The explanation of the observed⁷⁻¹² asymmetry in the reversal mechanism between the field increasing and field decreasing branches of the hysteresis loop remains one of the great challenges in these systems.

Of particular interest are the exchange bias properties in $(\text{La}, \text{Ca})\text{MnO}_3$ AF/FM bilayers and multilayers because they exhibit some distinct exchange coupling features¹³⁻¹⁵ relative to their transition-metal³ counterparts. Exchange biasing has been detected below a blocking temperature $T_B \approx 70$ K in bilayers¹⁵ and multilayers¹³ consisting of alternating FM and AF $(\text{La}, \text{Ca})\text{MnO}_3$ layers for a variety of Ca^{2+} concentrations.¹⁴ A distinct asymmetry of the magnetization reversal mechanism has been observed¹⁴ in (i) the magnetizing field dependence of the left (H_1) and right (H_2) coercive fields where the film magnetization goes to zero on the field decreasing and increasing branches of the loop respectively and (ii) the pronounced asymmetry in the field decreasing and increasing branches of isothermal magnetoresistance loops measured below T_B . This asymmetry disappears above T_B , indicating that it is related only with the exchange biasing mechanism.

The time dependence of the magnetization under a constant external field measures the thermal activation of the

magnetization over energy barriers, which define the magnetization process in a film and is usually applied for the study of the magnetization reversal mechanism. In FM films that exhibit a wide range of energy barriers the magnetization time decay follows a $\ln(t)$ behavior^{16,17} only below a blocking or freezing temperature T_f , resulting from the superposition of many exponential decays with different magnetic relaxation times. The slope of the magnetization time decay represents the *magnetic viscosity*: $S = -(\partial M / \partial \ln t)|_H$, which can be conveniently expressed in percent moment decay per decade.¹⁸ An irreversible change of the magnetization dM can be induced as well by a change of the external field by dH . Such changes define the irreversible susceptibility $\chi_{irr} = (\partial M / \partial H)|_t$. A fictitious field can be defined as well, which arises from thermal fluctuation effects¹⁹: $H_f = S / \chi_{irr}$. This H_f can be estimated by macroscopic measurements and can provide further insight into the magnetization reversal mechanism. In addition, it is used to evaluate the activation volume for the magnetization reversal¹⁹:

$$V^* = \frac{k_B T}{M_s H_f}. \quad (1)$$

However, the observed T_B in exchange-biased films is mainly associated with the stabilization of the unidirectional anisotropy at the FM/AF interfaces. Thus, on application of a field below T_B in AF/FM systems, the time dependence of the magnetization measures the thermal activation over energy barriers originating from the unidirectional anisotropy. Thus far, time dependence measurements on AF/FM systems have been explained by using different models.^{12,20,21} In MnF_2/Fe bilayers¹² the observed asymmetry of magnetization reversal is attributed to coherent rotation in the one loop side and to domain nucleation on the other loop side. In NiO/NiCoFe or $\text{FeMn}/\text{NiCoFe}$ bilayers²⁰ the observed decrease of $H_{EB}(t)$ has been interpreted as a thermally assisted reversal of the staggered magnetization directions of magnetic domains in the AF layer. For the case of the pinned $\text{FeMn}/\text{NiCoFe}$ layer of a spin-valve²¹ complex time-

dependent effects occur in the FM (pinned) layer due to significant reversal in the AF (pinning) layer during the time of measurement.

In this study the asymmetry of the reversal mechanism is probed by magnetic viscosity and remanence measurements in [(FM)La_{0.60}Ca_{0.40}MnO₃(4 nm)/(AF)La_{0.33}Ca_{0.67}MnO₃(4 nm)]₁₅ multilayers, where the maximum exchange biasing field (H_{EB}) is observed.¹⁴ The multilayers were prepared by pulsed laser deposition of bulk stoichiometric targets on (001)LaAlO₃ (LAO) single-crystal substrates. The beam of an LPX105 excimer laser (Lambda Physic), operating with KrF gas ($\lambda = 248$ nm), was focused on a rotating target. During deposition the substrate temperature was stabilized at 700 °C and the oxygen pressure in the chamber was 0.3 Torr, resulting in a deposition rate of 0.03 nm per pulse. The multilayers were grown on a 40-nm-thick La_{0.33}Ca_{0.67}MnO₃ AF buffer layer due to better lattice matching with the LAO substrate used.

The epitaxially strained growth of these multilayers has been revealed by low-angle and high-angle x-ray diffraction (XRD), conventional, and high-resolution transmission electron microscopy (TEM) measurements in previous studies.^{14,15} The XRD spectra show a strong texturing along the pseudocubic (001) direction of the perovskite unit cell. Both XRD and TEM measurements show that the out-of-plane d spacings are 0.382 nm for the AF (0.381 nm in bulk) and 0.390 nm (0.3858 nm in bulk) for the FM layers.¹⁵ This out-of-plane lattice expansion indicates that the FM layer carries a stress-induced anisotropy which adds to the total magnetic anisotropy energy. Since the magnetic easy axis is along the direction of tensile strain in strained (La,Ca)MnO₃ epitaxial films,²² the FM layers would exhibit an out-of-plane, stress-induced, uniaxial anisotropy.¹⁵ This anisotropy is revealed when isothermal magnetization and remanence measurements are compared with the field applied parallel (H_{\parallel}) and perpendicular (H_{\perp}) to the film plane, as indicated by experiments^{15,23} that study the reversal modes in exchange-biased AF/FM multilayers with an out-of-plane easy axis.

Magnetic relaxation measurements were performed in a Quantum Design MPMSR2 superconducting quantum interference device (SQUID) magnetometer. For these measurements [$M(t)$] the sample was initially saturated by field cooling (FC) in 50 kOe from 300 K to 5 K or 80 K. Subsequently the field was reduced to a constant value between 5 and -5 kOe, and the magnetization was measured as a function of time. During the $M(t)$ data collection the temperature was stabilized within 20 mK. To collect relaxation data for the field increasing branch the sample was exposed to -50 kOe after the field cooling in 50 kOe and then the field was fixed to the desired value where the $M(t)$ data were collected. Remanent magnetization $M_R(H)$ curves were obtained for the same fields and temperatures for which relaxation measurements were performed. Thus, for $M_R(H)$ measurements the multilayer was field cooled in 50 kOe, then the $M(H)$ magnetization was measured first at a field $5 \geq H \geq -5$ kOe, and subsequently the field was set to zero and the $M_R(H)$ was detected for the same fields. For the field increasing branch of the loop the sample was field cooled in

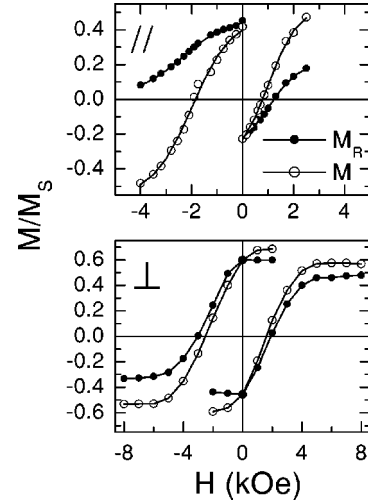


FIG. 1. $M(H)$ (open circles) and $M_R(H)$ (solid circles) curves at 5 K. The upper panel depicts longitudinal bias measurements and the lower panel perpendicular bias measurements.

50 kOe, then the field was reversed to -50 kOe, and the $M(H)$, $M_R(H)$ curves were measured as before.

Figure 1 shows $M(H)$ and $M_R(H)$ curves performed with H_{\parallel} and H_{\perp} at 5 K. In $M(H)$ curves with H_{\parallel} we observe a loop displacement $H_{EB}(\parallel) = -(H_1 + H_2)/2 = 0.64$ kOe, and a loop half-width $H_c(\parallel) = -(H_1 - H_2)/2 = 1.26$ kOe, whereas $H_c(\perp) = 2.1$ kOe, $H_{EB}(\perp) = 0.57$ kOe, and the M_R loop is more symmetric for H_{\perp} . These results show that the H_{\parallel} measurement is performed along a hard axis in the FM layers. It is worth noting that the $M_R(H)$ curves are very different from the $M(H)$ curves only for the H_{\parallel} case, exhibiting very high reversibility. In addition, the pronounced reversibility of the field decreasing branch of the loop leads to a very asymmetric remanence curve, with an H_1 exceeding 6 kOe, implying an extra contribution from the exchange bias field.

Magnetic relaxation measurements have been employed along with the remanence measurements to probe the asymmetry of the magnetization reversal for H_{\parallel} and H_{\perp} . Figure 2 shows typical $M(t)$ measurements at 5 K for the field increasing and field decreasing branches of the loop with H_{\parallel} . The field increasing branch is measured at $H = -1.5$ kOe and the field decreasing branch at $H = 1.0$ kOe, due to the loop shift. In both cases the magnetization exhibits a linear dependence with $\ln(t)$. This indicates that during the reversal in the FM layer there is no significant reversal in the AF layers which would lead to a variable exchange field acting on the FM domains.²¹ Similar $M(t)$ measurements were performed in various fields H to construct the $S(H)$ curves shown in Fig. 3 for H_{\parallel} and H_{\perp} . The $\chi_{irr}(H)$ was estimated from the first derivative of the S-shaped $M_R(H)$ curve, $dM_R(H)/dH$, and is shown in Fig. 3. Since we have used the percent of M_S moment change per decade of time units for $S(H)$, we express χ_{irr} in units normalized to M_S to obtain a direct estimation of the fluctuation field from their ratio¹⁸ $H_f = S(H)/[100 \ln(10) \chi_{irr}(H)]$. Both the $S(H)$ and $\chi_{irr}(H)$ curves are “bell shaped,” exhibiting their maxima in fields which are close to H_1 and H_2 coercivities (dotted vertical

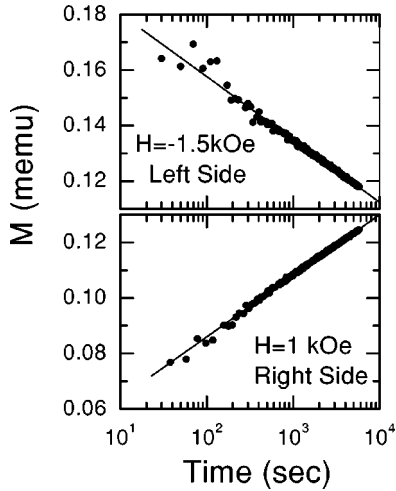


FIG. 2. Magnetization as a function of time for the field decreasing (upper panel) and field increasing (lower panel) branches of the loop. The measurements were performed at 5 K and the field was applied in the film plane.

lines). Such bell shaped curves are usually observed²⁴ in FM materials.

A marked difference (Fig. 4) between the H_{\parallel} and H_{\perp} measurements is the large asymmetry that appears only in $S(H)$ and $\chi_{irr}(H)$ curves for the field increasing and field decreasing branches of the loop with H_{\parallel} . This reflects the different potential barriers imposed to domain wall motion during the magnetization reversal from $+M$ to $-M$ and from $-M$ to $+M$ state in the two parts of the loop with H_{\parallel} . Another relaxation study¹² reports a small deviation from the $\ln(t)$ behavior and a sharp peak in $S(H)$ curves for the left loop side, both providing evidence for a rotation mechanism with a *small* distribution of barriers to reversal. In our results neither of these effects are observed. Figure 4 shows that for H_{\perp} the $H_f(V^*)$ curves exhibit a minimum near by the H_1 and H_2 coercivities which is reminiscent to that observed²⁵ in an

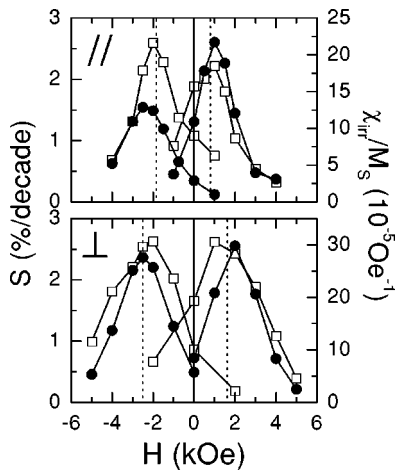


FIG. 3. Magnetic viscosity (open symbols) $S(H)$ and irreversible susceptibility $\chi_{irr}(H)$ curves at 5 K. Upper panel is for H_{\parallel} and lower panel for H_{\perp} . The dashed lines indicate the position of H_1 and H_2 coercivities.

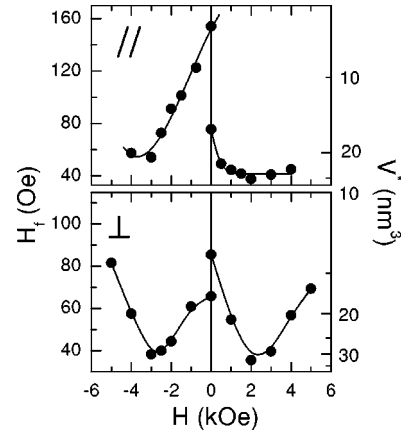


FIG. 4. Plots of the fluctuation field H_f and activation volume V^* as a function of the applied field. Upper panel is for H_{\parallel} and lower panel for H_{\perp} .

assembly of randomly oriented, single-domain particles where the magnetization reversal takes place by coherent rotation. However, it cannot be considered as unambiguous evidence for such a reversal mechanism. This similarity may arise from the strain-induced¹⁵ perpendicular anisotropy that dominates the magnetic reversal mechanism.

On the other hand, the H_{\parallel} measurement reveals that H_f exhibits a different field dependence between the two branches of the loop, where the relatively high H_f values give a smaller V^* (less than 30 nm^3) than for H_{\perp} . It is worth noting that the larger H_f values (or smaller V^*) with H_{\parallel} are obtained for the magnetization reversal from the $+M$ to $-M$ state, where the strength of the pinning forces is enhanced from the unidirectional anisotropy at the AF/FM interfaces. The obtained activation volume V^* has a typical size of about 20 nm^3 that results in a diameter of less than 4 nm if we consider domains with a spherical shape. This size fits well across a FM layer thickness and is comparable with a correlation length of a partial domain wall in exchange coupled AF/FM interfaces. It was shown²⁶ that Eq. (1) holds for single-domain particles or strong domain wall pinning whereas in the case of weak pinning this V^* is smaller by a factor of 2. In accordance, the obtained differences in activation volumes between the increasing and decreasing field parts of the loop (Fig. 4) suggest different reversal mecha-

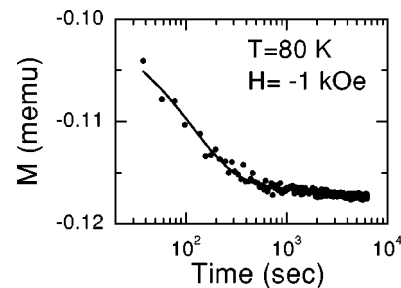


FIG. 5. Magnetization as a function of time at 80 K. A field of -1 kOe was applied in the film plane. The solid line is a fit with a function that includes a logarithmic and an exponential term.

nisms. Such differences between the increasing and decreasing field part of the loop may arise from the unidirectional anisotropy at the AF/FM interfaces¹¹ in longitudinal bias experiments.

In contrast to pure logarithmic time dependence of the magnetization at 5 K (Fig. 2) the $M(t)$ decay at 80 K shows a different behavior (Fig. 5). The data in Fig. 5 can be fitted with a function that includes logarithmic and exponential decay terms,²⁷ as expected¹⁶ for $M(t)$ measurements above T_B . The major contribution originates from the exponential component which accounts for the 70% of the total magnetization decay within the observed time window. However, the coexistence of two time decay components does not allow a reliable estimation of V^* values above T_B .

In summary, it was shown that the $S(H)$ and $\chi_{irr}(H)$ curves differ substantially between the longitudinal and perpendicular bias experiments due to strain-driven perpendicular anisotropy in the multilayer. Both curves exhibit a large asymmetry between the increasing and decreasing field parts of a loop in longitudinal bias experiments, evidencing two inequivalent reversal mechanisms. However, the $S(H)$ and $\chi_{irr}(H)$ curves are symmetric in perpendicular bias experiments, indicating that the equivalent reversal modes appear in the increasing and decreasing field parts of a loop due to the strong contribution of the perpendicular anisotropy. Finally, the dominance of an exponential $M(t)$ decay above T_B reveals a crossover between the $\ln(t)$ law when the exchange bias sets in and the exponential relaxation when H_{EB} vanishes.

-
- ¹A. Gupta and J.Z. Sun, *J. Magn. Magn. Mater.* **200**, 24 (1999).
²C. Christides, in *Handbook of Surfaces and Interfaces*, edited by H. S. Nalwa (Academic Press, New York, 2001), Vol. 4, Chap. 2, p. 77.
³J. Nogues and I.K. Schuller, *J. Magn. Magn. Mater.* **192**, 203 (1999).
⁴C.H. Tsang, R.E. Fontana, Jr., T. Lin, D.E. Heirn, B.A. Gurney, and M.L. Williams, *IBM J. Res. Dev.* **42**, 103 (1998).
⁵J. Nogues, T.J. Moran, D. Lederman, I.K. Schuller, and K.V. Rao, *Phys. Rev. B* **59**, 6984 (1999).
⁶N.J. Gokemeijer, R.L. Penn, D.R. Veblen, and C.L. Chien, *Phys. Rev. B* **63**, 174422 (2001).
⁷V.I. Nikitenko, V.S. Gornakov, L.M. Dedukh, Yu.P. Kabanov, A.F. Khapikov, A.J. Shapiro, R.D. Shull, A. Chaiken, and R.P. Michel, *Phys. Rev. B* **57**, 8111 (1998).
⁸M.D. Stiles and R.D. McMichael, *Phys. Rev. B* **60**, 12950 (1999); **59**, 3722 (1999).
⁹V.I. Nikitenko, V.S. Gornakov, A.J. Shapiro, R.D. Shull, Kai Liu, S.M. Zhou, and C.L. Chien, *Phys. Rev. Lett.* **84**, 765 (2000).
¹⁰J. Wang, W.N. Wang, X. Chen, H.W. Zhao, J.G. Zhao, and W.Sh. Zhan, *Appl. Phys. Lett.* **77**, 2731 (2000).
¹¹M.R. Fitzsimmons, P. Yashar, C. Leighton, I.K. Schuller, J. Nogues, C.F. Majkrzak, and J.A. Dura, *Phys. Rev. Lett.* **84**, 3986 (2000).
¹²C. Leighton and I.K. Schuller, *Phys. Rev. B* **63**, 174419 (2000); C. Leighton, M.R. Fitzsimmons, P. Yashar, A. Hoffmann, J. Nogues, J. Dura, C.F. Majkrzak, and I.I. Schuller, *Phys. Rev. Lett.* **86**, 4394 (2001).
¹³I. Panagiotopoulos, C. Christides, M. Pissas, and D. Niarchos, *J. Appl. Phys.* **85**, 4913 (1999); *Phys. Rev. B* **60**, 485 (1999).
¹⁴N. Moutis, C. Christides, I. Panagiotopoulos, and D. Niarchos, *Phys. Rev. B* **64**, 094429 (2001).
¹⁵C. Christides, N. Moutis, Ph. Komninou, Th. Kehagia, and G. Nuet, *J. Appl. Phys.*, (to be published).
¹⁶E. M. Chudnovsky and J. Tejada, in *Macroscopic Quantum Tunneling of the Magnetic Moment* (Cambridge University Press, Cambridge, England, 1998), Chap. 5.
¹⁷R. Street and S.D. Brown, *J. Appl. Phys.* **76**, 6386 (1994).
¹⁸S.M. Stinnett, W.D. Doyle, O. Koshkina, and L. Zhang, *J. Appl. Phys.* **85**, 5009 (1999).
¹⁹A. Lyberatos and R.W. Chantrell, *J. Phys.: Condens. Matter* **9**, 2623 (1999).
²⁰P.A.A. van der Heijden, T.F.M.M. Maas, W.J.M. de Jonge, J.C.S. Kools, F. Roozeboom, and P.J. van der Zaag, *Appl. Phys. Lett.* **72**, 492 (1998).
²¹A.M. Goodman, H. Laidler, K. O'Grady, N.W. Owen, and A.K. P-Long, *J. Appl. Phys.* **87**, 6409 (2000).
²²T.K. Nath, R.A. Rao, D. Lavric, C.B. Eom, L. Wu, and F. Tsui, *Appl. Phys. Lett.* **74**, 1615 (1999).
²³S. Maat, K. Takano, S.S.P. Parkin, and E.E. Fullerton, *Phys. Rev. Lett.* **87**, 087202 (2001).
²⁴I.D. Mayergoyz, A. Adly, C. Korman, M. Huang, and C. Krafft, *J. Appl. Phys.* **85**, 4358 (1999).
²⁵A.M. de Witte, K. O'Grady, G.N. Coverdale, and R.W. Chantrell, *J. Magn. Magn. Mater.* **88**, 183 (1990).
²⁶P. Gaunt, *J. Appl. Phys.* **59**, 4129 (1986).
²⁷M. Sirena, L.B. Steven, and J. Guimpel, *Phys. Rev. B* **64**, 104409 (2001).